2018 AIUM Annual Convention

Reverberant Shear Wave Elastography (R-SWE)

Implementation and feasibility studies

Juvenal Ormachea and Kevin Parker

University of Rochester

Rochester, NY, USA.

UNIVERSITY of ROCHESTER

Elastography, what are the problems?

- Presence of reflected waves from organ boundaries and internal inhomogeneities

- **Cause** modal patterns in continuous wave applications
  backwards traveling waves in transient wave experiments.
- **Result** biased estimates of shear wave speed (SWS)

  → conventional methods assume shear wave propagation ***parallel to the lateral direction***

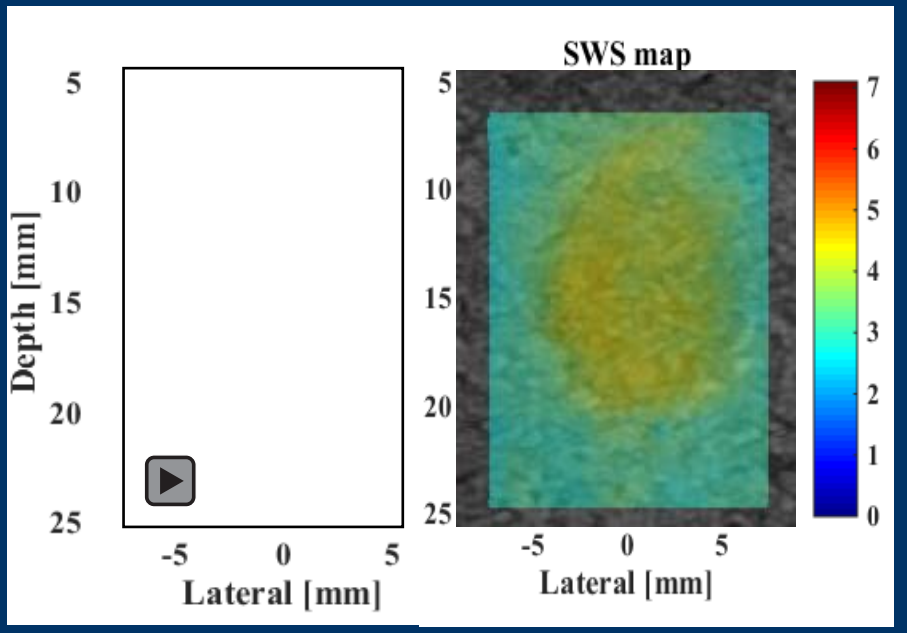

Data from LogiqE9 system

Elastography, what are the problems?

- Presence of reflected waves from organ boundaries and internal inhomogeneities
- Solutions: Directional filters

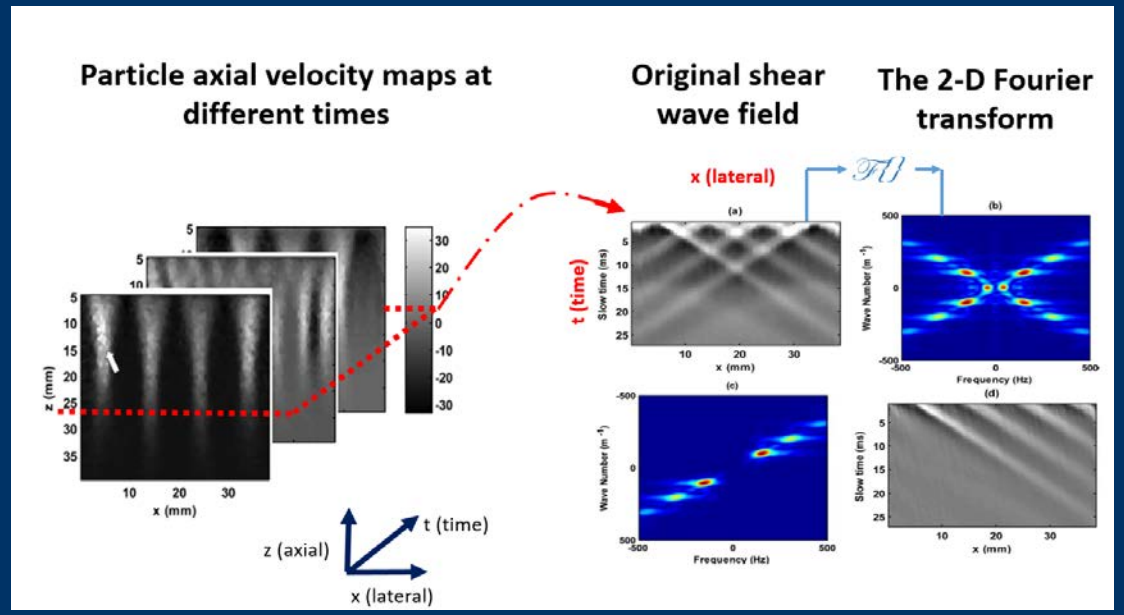

Song et al. (2015)

Particle axial velocity movie

Filtered data movie

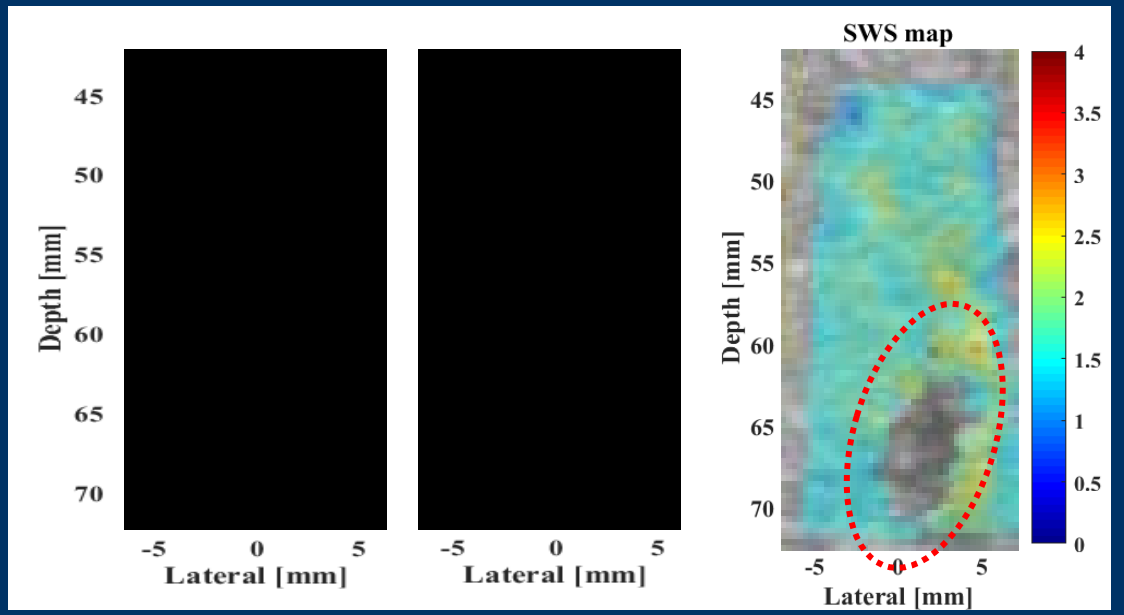

Data from LogiqE9 system

Elastography, what are the limitations?

Penetration

- Liver -> Obesity, ascites
- Prostate -> 3-4cm. In large prostate, not deep enough to measure anterior zone
- Thyroid -> about 5.5cm. Large and deeply nodules cannot be properly assessed.

Shear wave propagation

- Breast -> Accuracy differs, problems with propagation of vibration energy. Weak in hard lesions

Pure gelatin based phantom:
Good shear wave penetration and propagation

Gelatin + 6% castor oil:
Problems with shear wave penetration and propagation

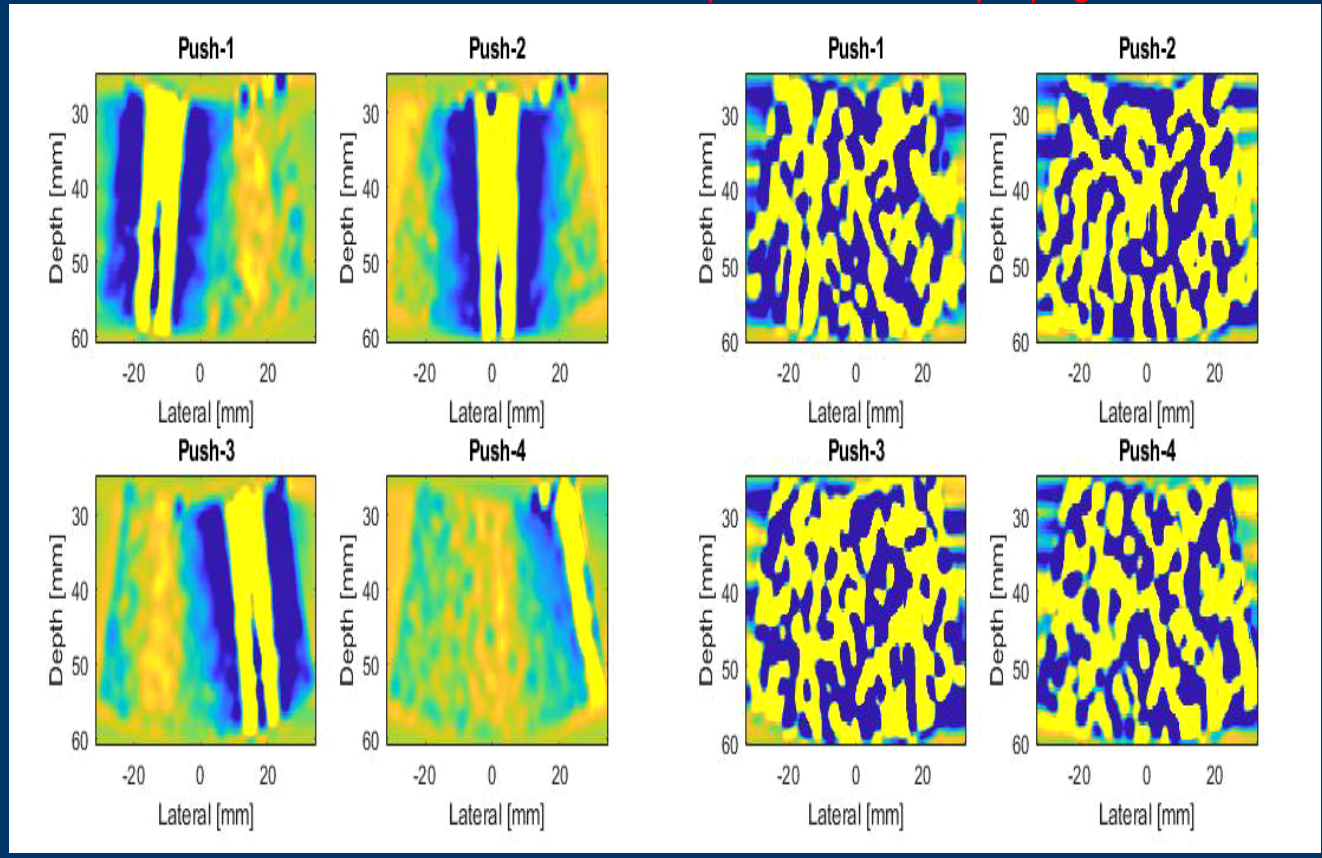

WFUMB guidelines and recommendations articles

Data from Samsung RS85 system

Motivation

- **Reflections**
- **Multiple waves**

→ **Are they *good* or *bad* for shear wave measurements?**

- **Penetration with good shear waves signals**

→ **How can we achieve it?**

Reverberant Shear Wave Elastography

- Shear waves of random amplitude and phase propagates in all directions as a statistically isotropic distribution across 4π steradians (Parker et al., 2017. Ormachea et al., 2018.)

- *Practically speaking, all tissue boundaries with reflections, and sources in the vicinity of the observation point contribute to the overall distribution.*

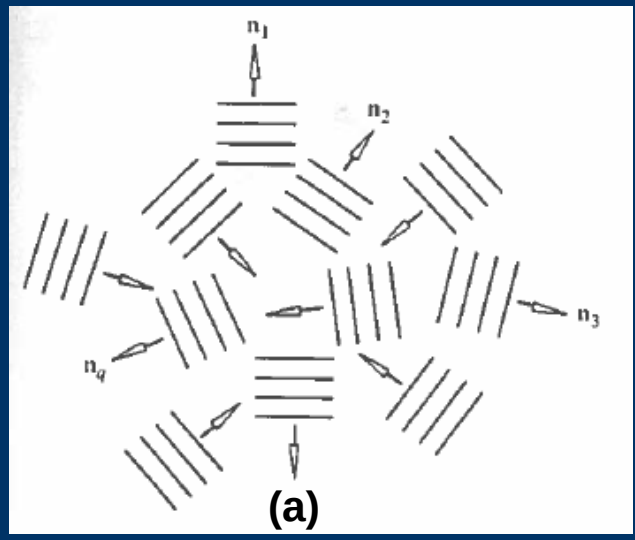

Historical framework from *Acoustics*
(A.D. Pierce, McGraw-Hill: New York, 1981, p. 257):

Reverberant Shear Wave Elastogography

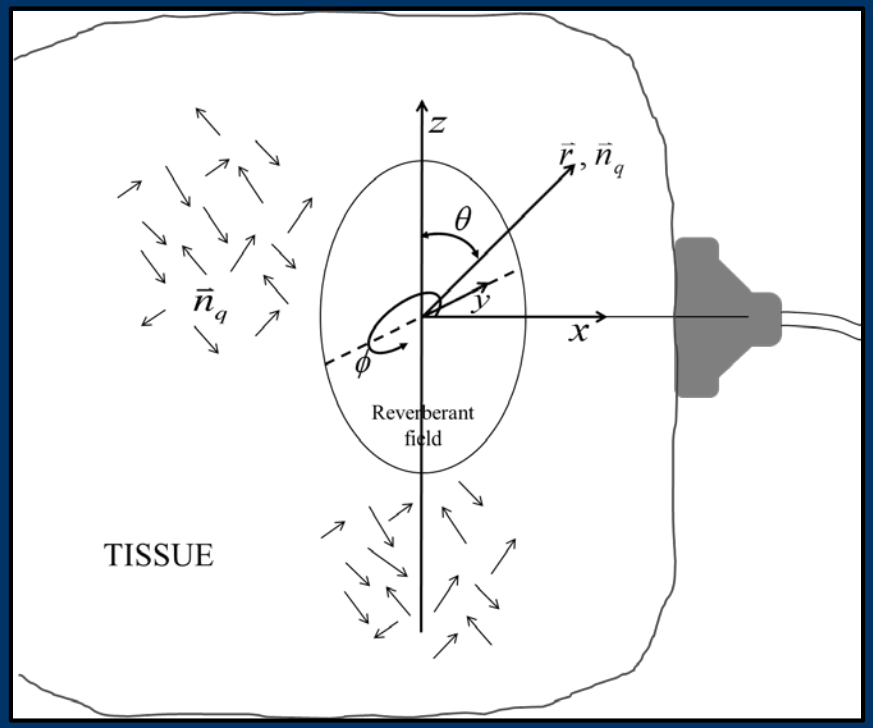

Schematic for the orientation of the imaging transducer and the object that has an isotropic random distribution of shear waves.

Parker et al. (2017)

- The monochromatic reverberant field pressure $\hat{P}$ at position $\boldsymbol{\varepsilon}$ and time t is:

$$\hat{P}(t,\boldsymbol{\varepsilon}) = \sum_q \hat{P}_q \exp\left[j\left(k\mathbf{n}_q \cdot \boldsymbol{\varepsilon} - \omega_0\right)t \right]$$

where

n_q : unit vectors in the direction of propagation of the q_{th} wave

$\hat{P}_q$: independent, identically distributed variables of random magnitude and phase.

Reverberant Shear Wave Elastography

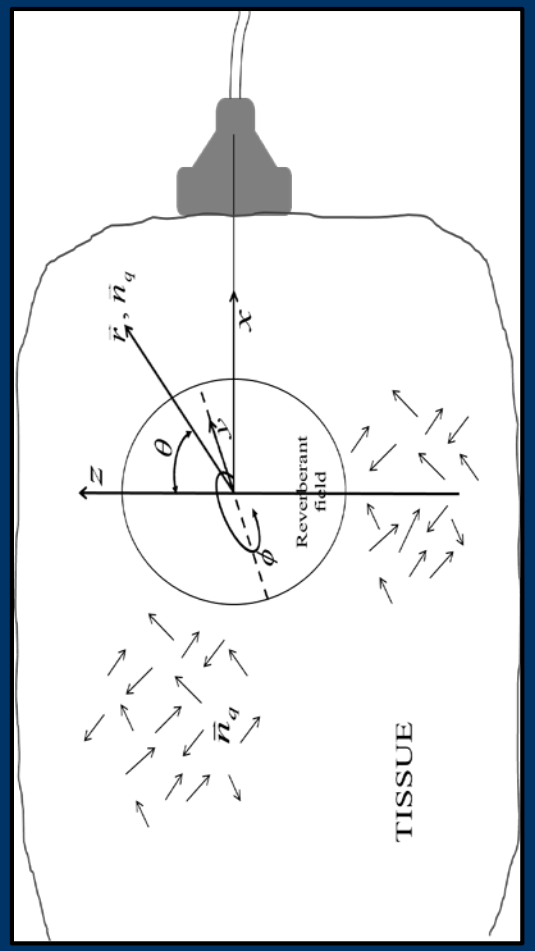

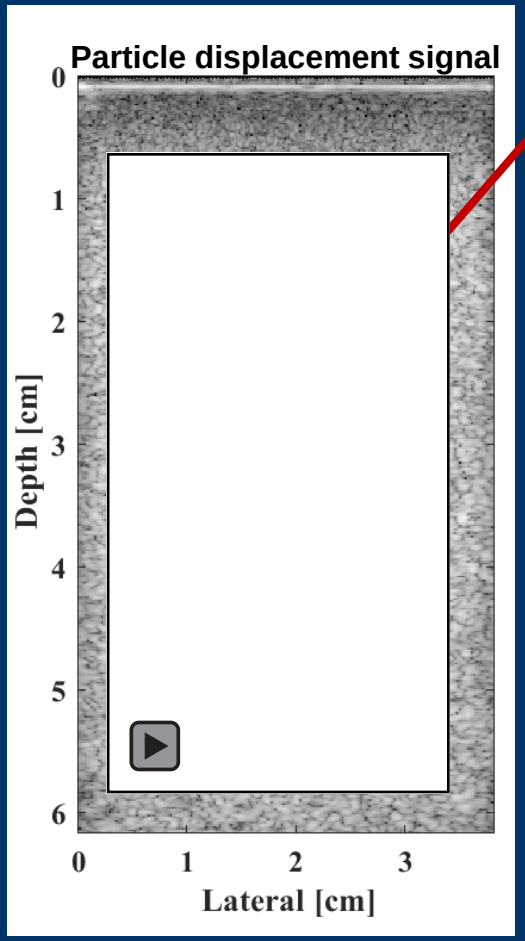

$$B v_x v_x(\Delta t, \Delta \varepsilon) = E\left\{\hat{v}_x(t,\varepsilon)\hat{v}_x^*(t+\Delta t, \varepsilon+\Delta\varepsilon)\right\}$$

Define the autocorrelation function of the detected shear wave velocity v_x

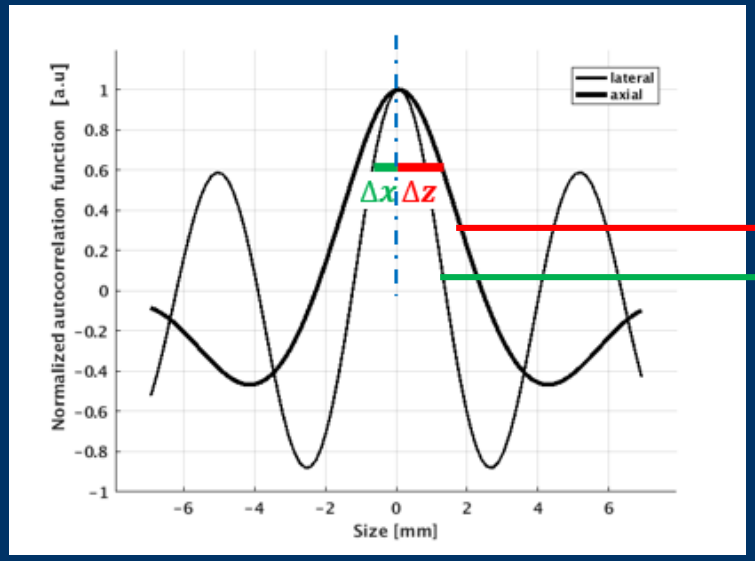

Autocorrelation profiles respect to:

- Axial direction
- Lateral direction

$$\left|\hat{k}_x\right|^2 = \frac{5}{\sqrt{2\pi}} \times \left(Re\{B_{vv}(0)\} - Re\{B_{vv}(\Delta x)\}\right),$$

$$\left|\hat{k}_z\right|^2 = 5 \times \left(Re\{B_{vv}(0)\} - Re\{B_{vv}(\Delta z)\}\right),$$

Wavenumber from autocorrelation functions

Reverberant Shear Wave Elastography

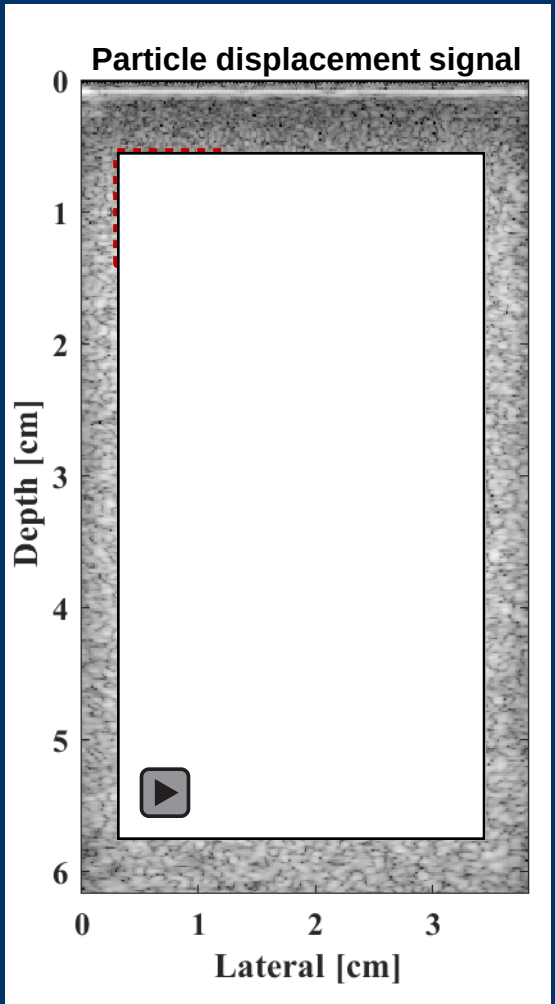

Final wavenumber

$$k = \sqrt{\frac{\hat{k}_x^{\,2} + \hat{k}_z^{\,2}}{2}}$$

Final shear wave speed

$$c_s = \frac{2\pi f_v}{k}$$

f_v: Vibration frequency
k: Wavenumber

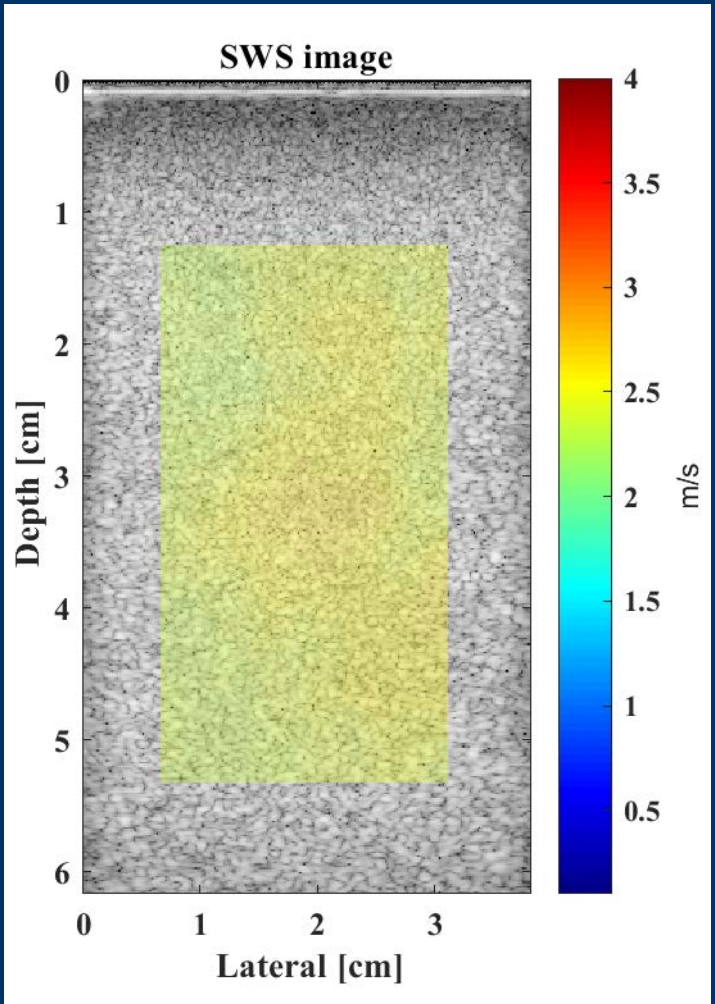

Experiments

CIRS breast phantom

Elastic modulus 20 kPa

CIRS viscoelastic ph.

Elastic modulus 6 kPa

- A Verasonics ultrasound system & linear ultrasound transducer L7-4, center frequency was 5 MHz
- Phantom materials:
  - CIRS breast phantom
  - CIRS viscoelastic phantom
- Vibration frequencies:
  - [60 to 450] Hz, CIRS breast phantom
  - [60 to 220] Hz, CIRS viscoelastic ph.

Results: CIRS breast phantom – Single frequencies

180Hz **220Hz** **360Hz** **450Hz**

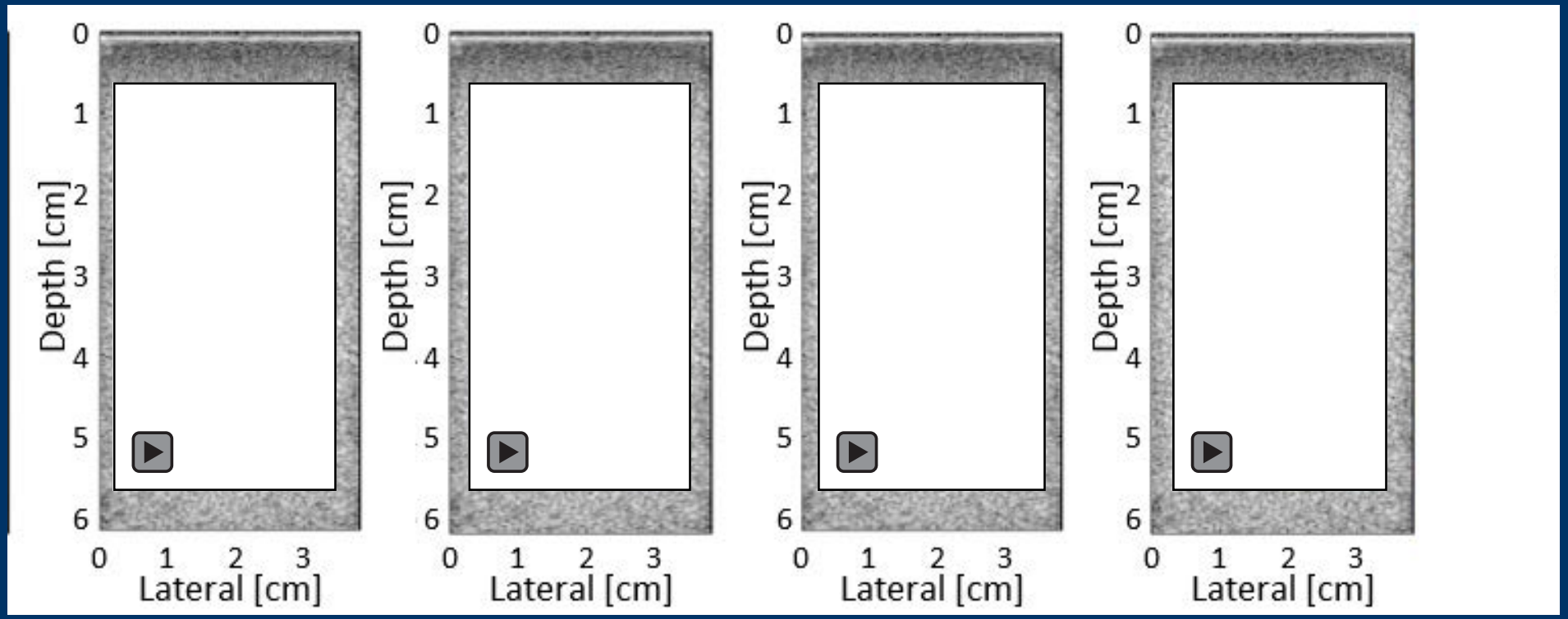

Particle displacement signals

Results: CIRS breast phantom – Multi frequencies

140-180-220Hz **300-360-400Hz** **400-450-500Hz**

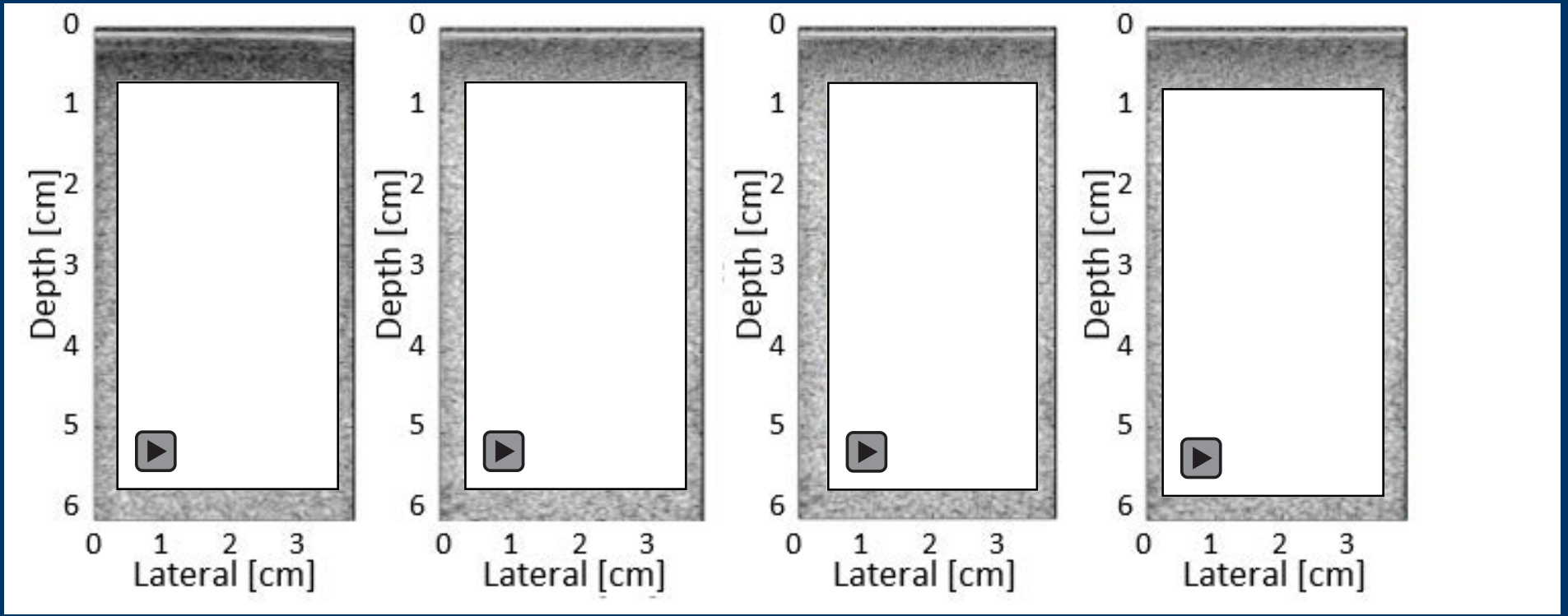

Particle displacement signals

Results: CIRS viscoelastic phantom – Single frequencies

100Hz **140Hz** **180Hz** **220Hz**

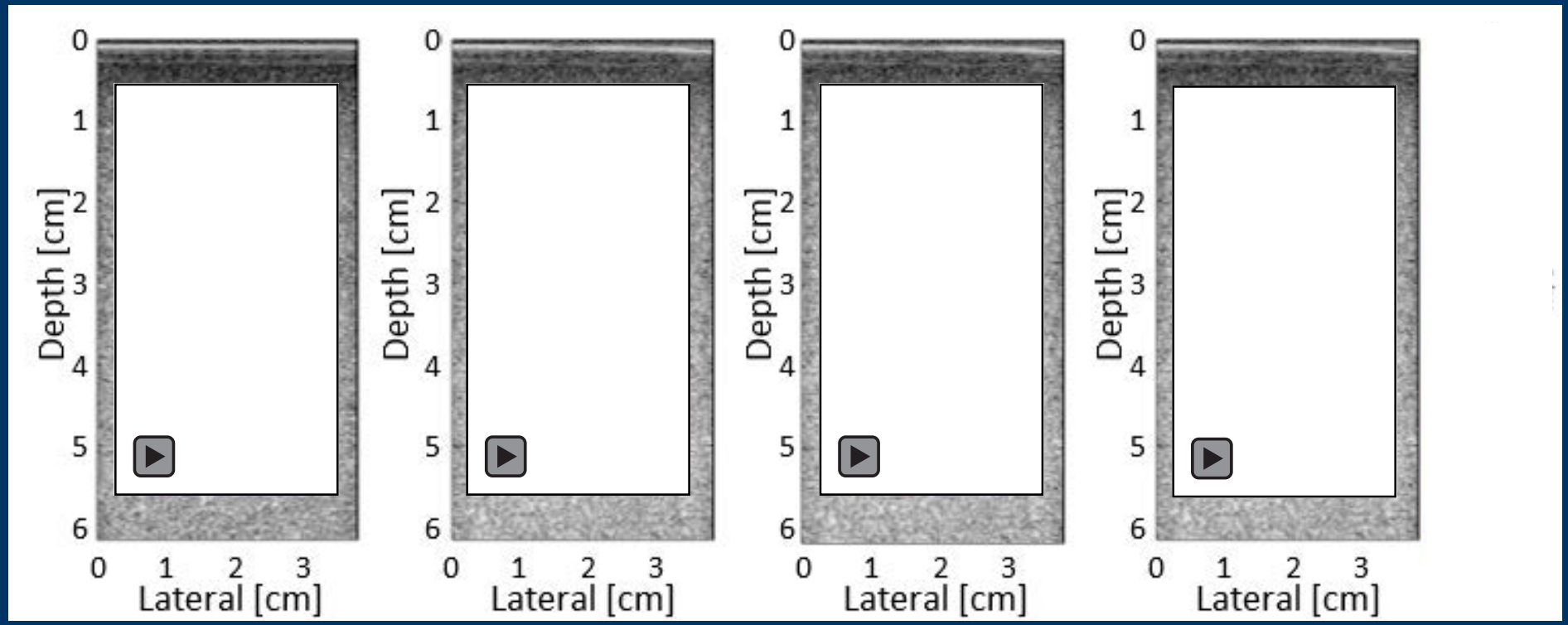

Particle displacement signals

Results: CIRS viscoelastic phantom – Multi frequencies

60-100-140Hz **100-140-180Hz** **140-180-220Hz**

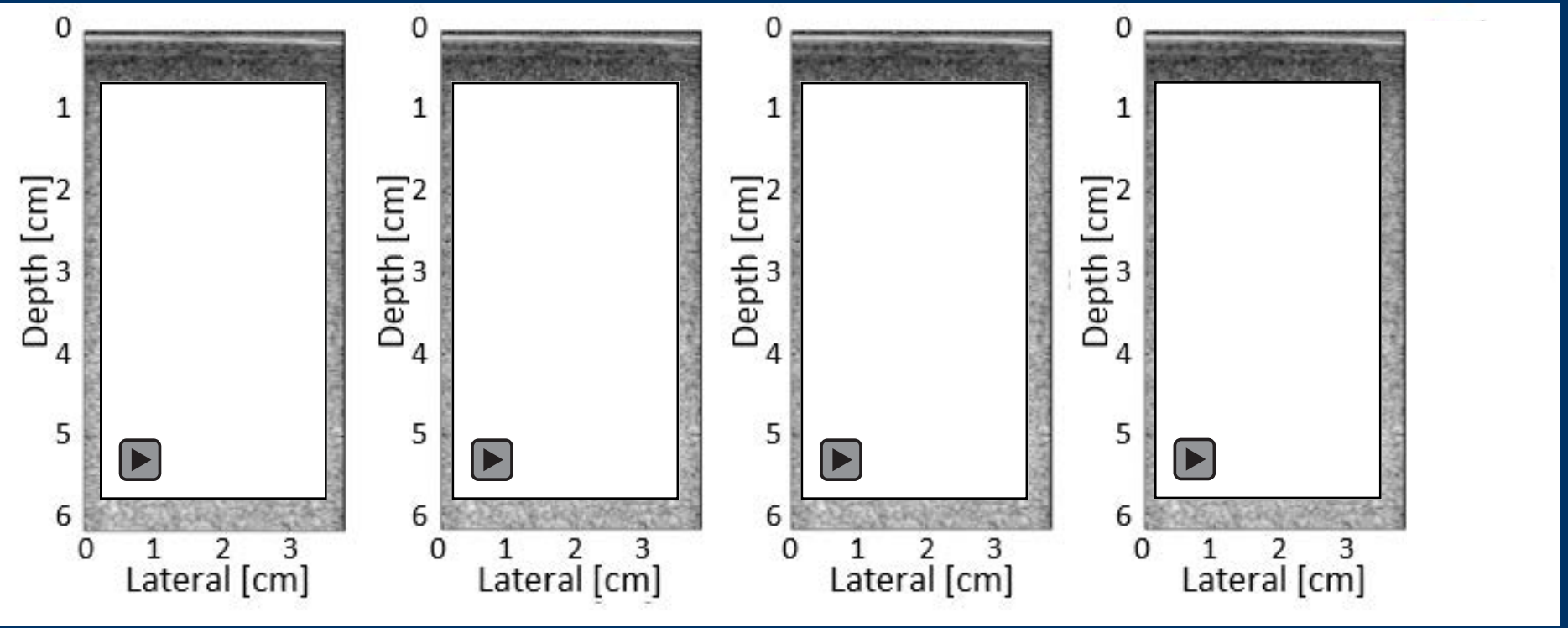

Particle displacement signals

Shear wave speed vs. Frequency

CIRS Breast phantom

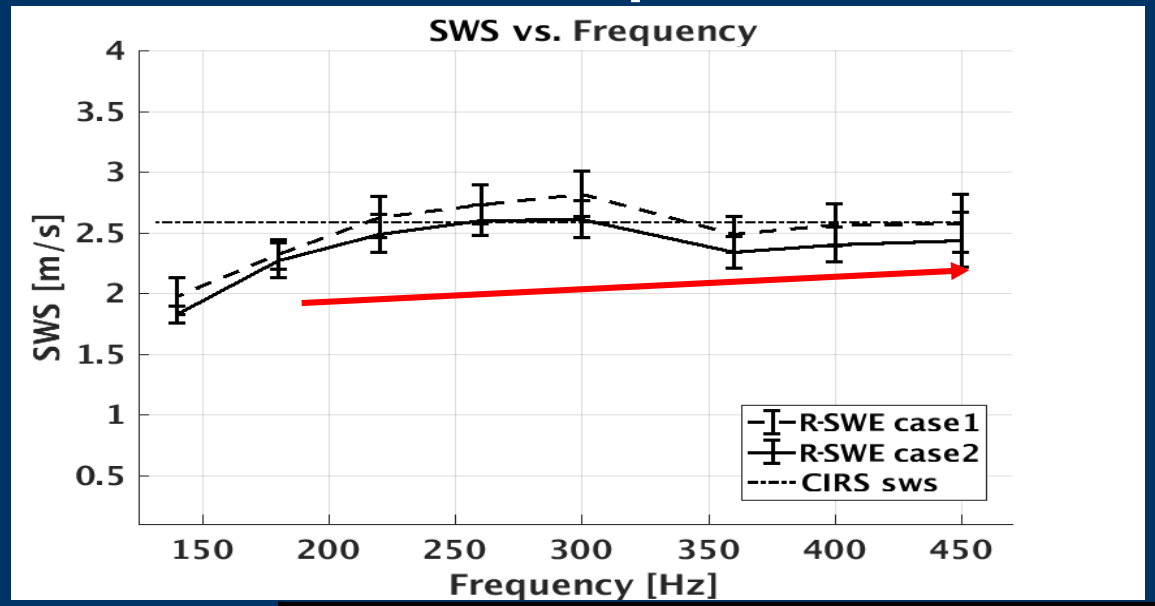

CIRS viscoelastic phantom

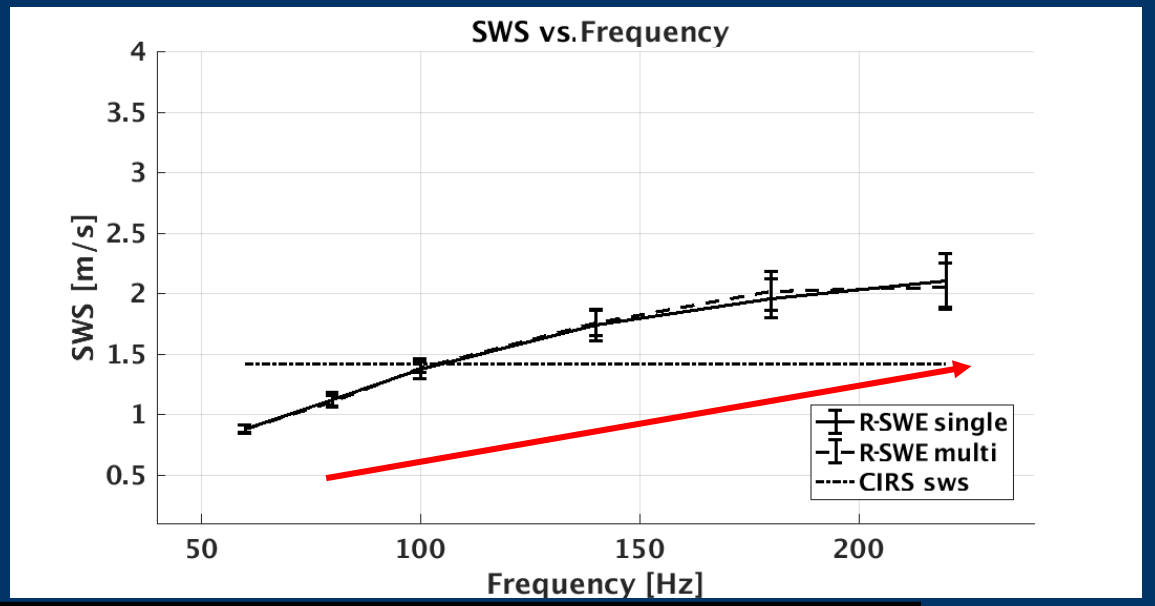

Dispersion (m/s/100Hz) values			
Phantom	**Experiment**	**Dispersion**	**Frequency range**
CIRS breast	Single	0.28	180-300 Hz
	Multi	0.32	
CIRS viscoelastic	Single	0.59	100-220 Hz
	Multi freq.	0.56	

Comparison with another SWE modality

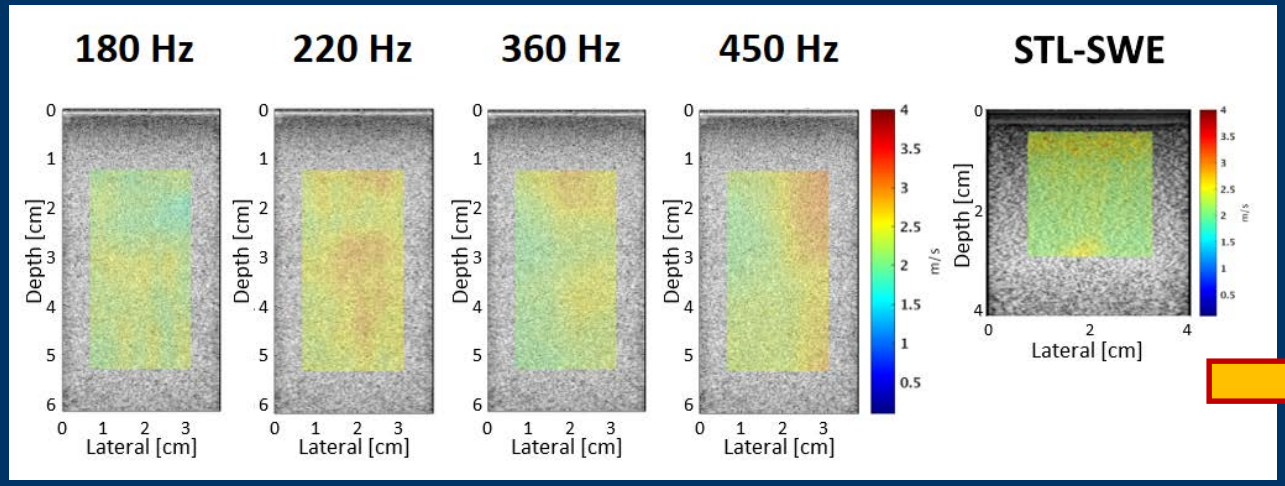

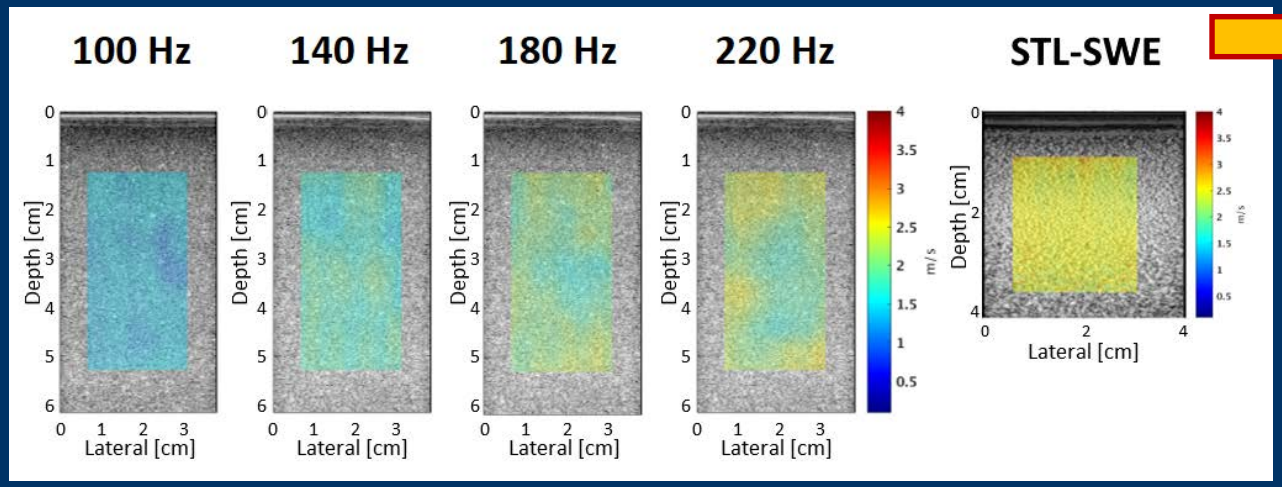

Difference with respect to STL-SWE at 220 Hz		
	Single	**Multi**
CIRS Breast	11.06 %	13.29%
CIRS viscoelastic	4.10%	5.94%

STL-SWE = single-tracking location shear wave elastography

Results: CIRS breast phantom – Inclusion region

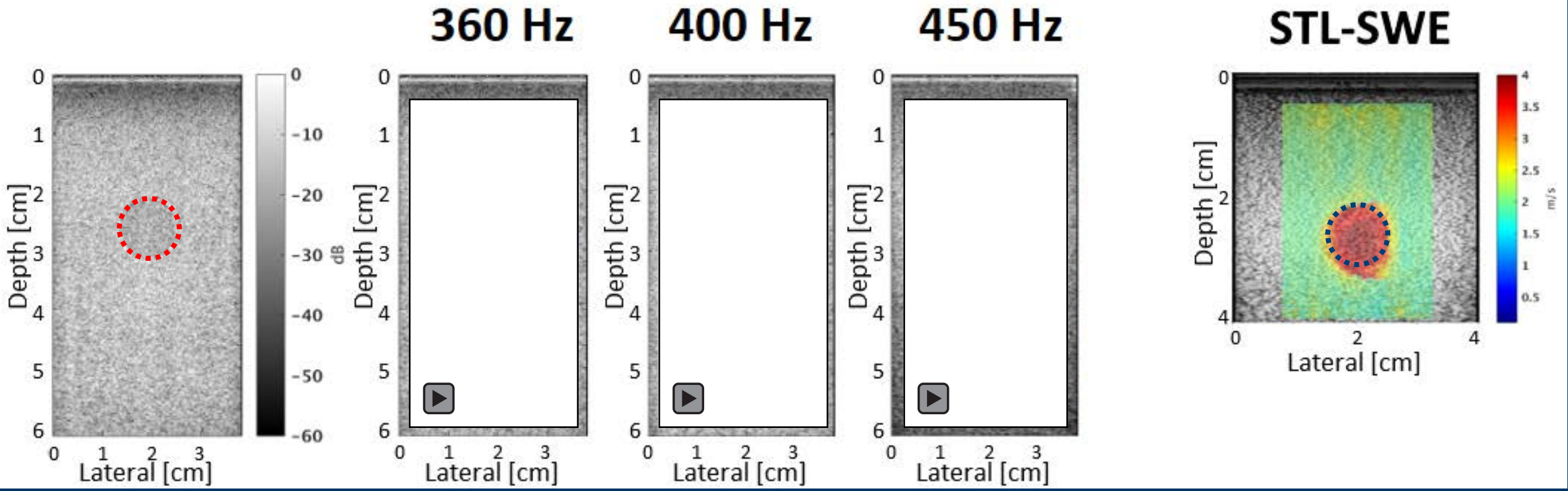

$$\text{contrast} = \frac{|\bar{c}_{in} - \bar{c}_{out}|}{\bar{c}_{out}}$$

$$\text{CNR} = \frac{|\bar{c}_{in} - \bar{c}_{out}|}{\sqrt{\sigma_{in}^2 + \sigma_{out}^2}}$$

Particle displacement signals

Contrast and Contrast to noise ratio (CNR)

	360 Hz	400 Hz	450 Hz	STL-SWE
Contrast	0.12	0.19	0.29	0.91
CNR	1.41	2.78	4.40	8.75

Results: *In vivo* human liver

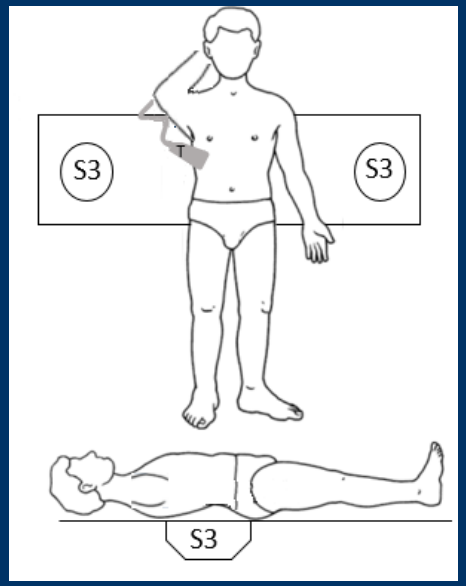

Patient were laid supine on a custom bed and the right arm abducted.

- A Verasonics ultrasound system & linear ultrasound transducer L7-4, center frequency was 5 MHz
- A volunteer patient for *in vivo* liver tissue.
- Vibration frequencies:
  - [40 to 240] Hz
- Scans under the requirements of informed consent and the University of Rochester Institutional Review Board

Results: *In vivo* human liver

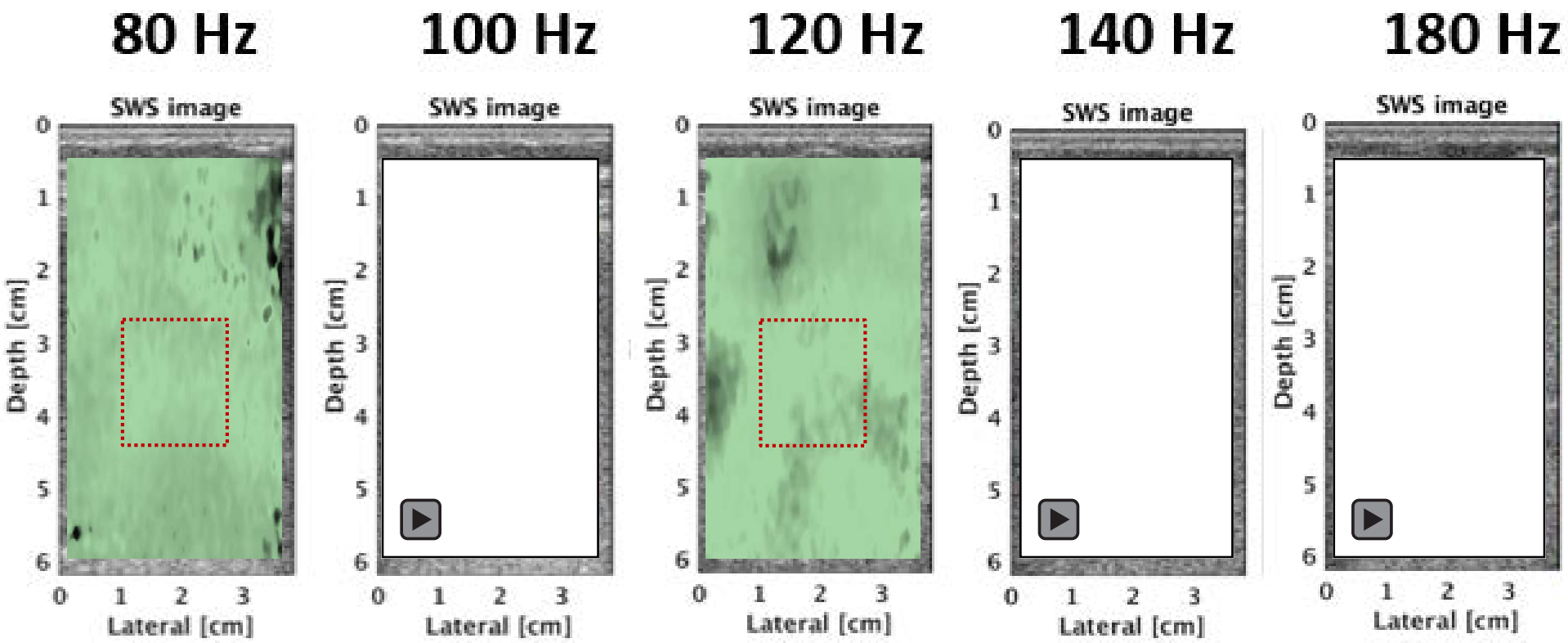

Particle displacement signals

Results: *In vivo* human liver

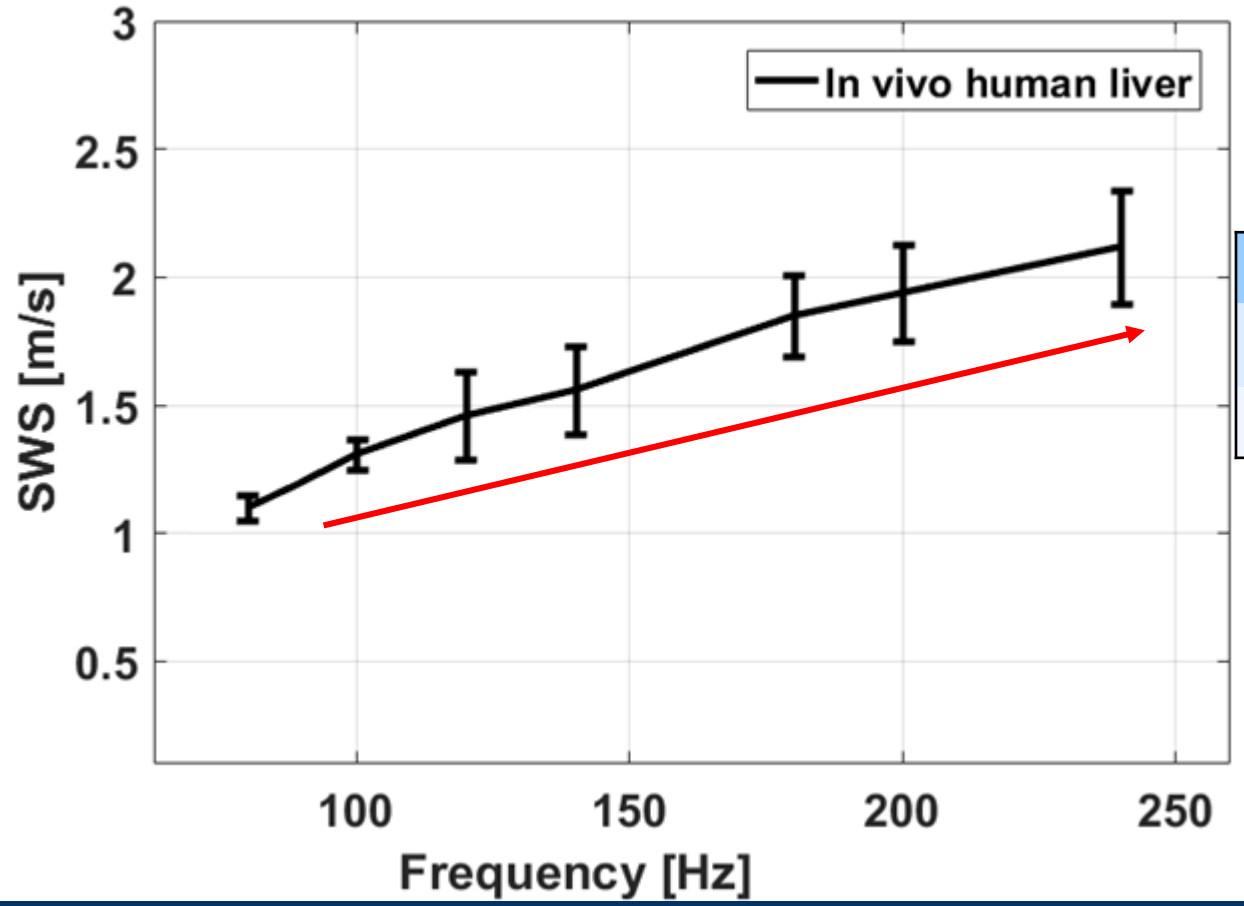

Dispersion (m/s/100Hz) values			
	Experiment	**Dispersion**	**Frequency range**
In vivo liver	Single	0.63	80-240 Hz

Preliminary results multi-frequencies: *In vivo* liver

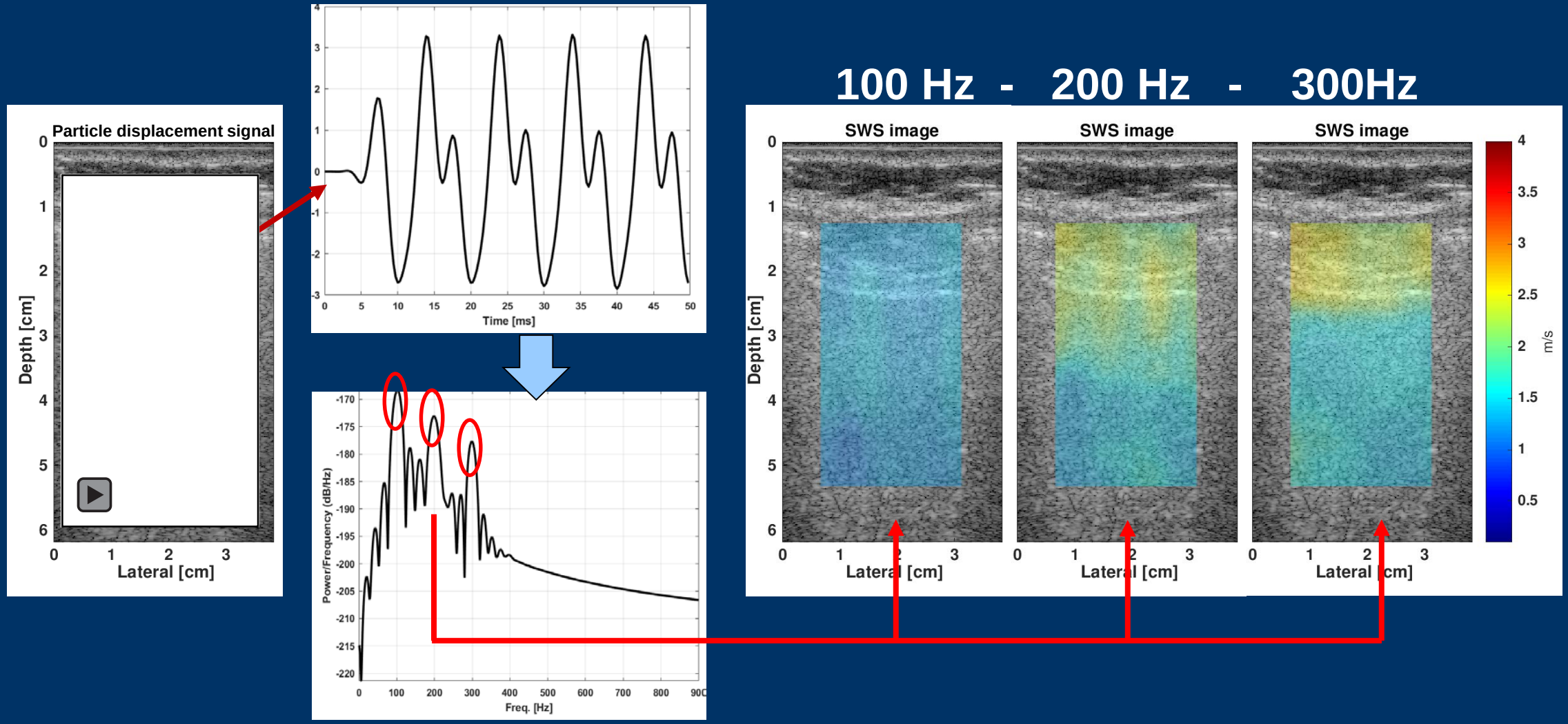

Summary

- CIRS breast phantom -> lower dispersion than CIRS viscoelastic → Expected since the viscoelastic phantom is a more dispersive media.
- No significant differences between single and multi-frequencies. → Approach is feasible and can more quickly assess tissue properties.
- Unlike other modalities, R-SWE does not filter or select for SWs propagation directions →
  - Facilitates the use for clinical applications.
  - Implementation is faster and simpler.

Summary

- The linear slope is comparable with results obtained with MRE (i.e. 0.75 m/s/100Hz at 25 Hz - 63 Hz (Klatt et al., 2007)) → However, the frequency ranges are different and cannot be strictly compared
- An ideal reverberant field is obtained using multiple sources around the ROI. → However, reflections from boundaries and in homogeneities help to randomize the field in practice.
- Tissue boundaries and inhomogeneities produce more reflection waves → Condition that is needed to create a reverberant field. Determination of shear wave sources is left for future research.

Summary

- Practical issue for clinicians concerns: time required for acquisition and processing of images

  → High frame rate ultrasound scanning, high complexity shear wave algorithms are already implemented. Limiting factor integration vibration sources with the ultrasound system

- A future study will apply R-SWE at a deeper region in fatty patients.

  → Further study will involve the viscoelastic property estimation

Conclusion

- It was possible to estimate the viscoelastic properties in phantom materials and in vivo human tissue using the R-SWE approach.
- Consistent SWS estimation that enables characterization and differentiation of elastic and viscoelastic materials.
- Multifrequency approach shows that it is feasible and can more quickly assess the frequency dependence of SWS.

Acknowledgments

- This work was supported by the Hajim School of Engineering and Applied Sciences at the University of Rochester.

- Juvenal Ormachea was supported by Peruvian Government scholarship 213-2014-FONDECYT.

Thank you

References

- Parker KJ, Ormachea J, Zvietcovich F, Castaneda B. Reverberant shear wave fields and estimation of tissue properties. Physics in medicine and biology, 2017;62:1046.
- Ormachea J, Castaneda B, Parker KJ. Shear wave speed estimation using reverberant shear wave fields: implementation and feasibility studies. Ultrasound in Medicine and Biology in press;
- Pierce A D 1981 McGraw-Hill Series in Mechanical Engineering (New York: McGraw-Hill)
- Song, P., Macdonald, M., Behler, R., Lanning, J., Wang, M., Urban, M., ... & Greenleaf, J. Two-dimensional shear-wave elastography on conventional ultrasound scanners with time-aligned sequential tracking (TAST) and comb-push ultrasound shear elastography (CUSE). Ultrasonics, Ferroelectrics, and Frequency Control, IEEE Transactions on, 2015; 62(2), 290-302.
- Barr RG., et al. WFUMB guidelines and recommendations for clinical use of ultrasound elastography: Part 2: breast. Ultrasound in Medicine and Biology, 2015, vol. 41, no 5, p. 1148-1160.
- Ferraioli G, et al. WFUMB guidelines and recommendations for clinical use of ultrasound elastography: Part 3: liver. Ultrasound in Medicine and Biology, 2015, vol. 41, no 5, p. 1161-1179.
- Cosgrove D, et al. WFUMB guidelines and recommendations on the clinical use of ultrasound elastography: Part 4. Thyroid. Ultrasound in Medicine and Biology, 2017, vol. 43, no 1, p. 4-26.
- Barr RG., et al. WFUMB guidelines and recommendations on the clinical use of ultrasound elastography: Part 5. Prostate. Ultrasound in Medicine and Biology, 2017, vol. 43, no 1, p. 27-48.